12th International Symposium on Turbulence and Shear Flow Phenomena (TSFP12)
Osaka, Japan (Online), July 19-22, 2022

SCALE-SPACE ENERGY DENSITY AND INHOMOGENEOUS EFFECT IN TURBULENT CHANNEL FLOW

Fujihiro Hamba
Institute of Industrial Science
The University of Tokyo
Komaba, Meguro-ku Tokyo 153-8505, Japan
hamba@iis.u-tokyo.ac.jp

ABSTRACT

A new expression for the scale-space energy density based on filtered velocities was proposed to clarify the reason for the negative value of the energy density and to better understand and predict inhomogeneous turbulent flows. The new expression consists of homogeneous and inhomogeneous terms; the former is always non-negative whereas the latter can be negative because of the turbulence inhomogeneity. DNS data of turbulent channel flow was used to examine the two terms of the turbulent energy and energy density. It was shown that a concave profile of the turbulent energy near the wall accounts for the negative value of the energy density very close to the wall.

INTRODUCTION

For homogeneous isotropic turbulence, the energy spectrum is commonly used to describe the scale dependence of turbulent fluctuations. The energy transfer has been studied in detail, and several closure theories have been developed. In contrast, one-point statistical quantities are mainly employed for inhomogeneous turbulence, such as the turbulent kinetic energy. The scale dependence of the energy must be important for understanding and predicting inhomogeneous turbulent flows.

The velocity field is decomposed into mean and fluctuating parts.

$$u_i^*(\mathbf{x}) = U_i(\mathbf{x}) + u_i(\mathbf{x}), \quad U_i = \langle u_i^* \rangle \tag{1}$$

For homogeneous turbulence, the Fourier transform is used to describe the scale dependence of the velocity fluctuation as follows:

$$u_i(\mathbf{x}) = \int d\mathbf{k} u_i(\mathbf{k}) \exp(i\mathbf{k}\cdot\mathbf{x}), \quad \int d\mathbf{k} = \int_{-\infty}^{\infty} dk_x \int_{-\infty}^{\infty} dk_y \int_{-\infty}^{\infty} dk_z \tag{2}$$

$$\langle u_i^2 \rangle = \int d\mathbf{k} Q_{ii}(\mathbf{k}), \quad \langle u_i(\mathbf{k}) u_i^\dagger(\mathbf{k}) \rangle = Q_{ii}(\mathbf{k}) \delta(\mathbf{0}) \tag{3}$$

The velocity fluctuation $u_i(\mathbf{x})$ is decomposed into Fourier modes in the wavenumber space in (2). Moreover, the velocity variance $\langle u_i^2 \rangle$ is also decomposed in the wavenumber space in (3). As a result, the turbulent kinetic energy $K(=\langle u_i^2 \rangle / 2)$ is expressed in terms of the energy spectrum as follows:

$$K = \int_0^\infty dk E(k) \tag{4}$$

$$E(k)[= 2\pi k^2 Q(\mathbf{k})] \geq 0 \tag{5}$$

The spectrum $E(k)$ can be considered an energy density in the wavenumber space and its integral is equal to the kinetic energy K. Moreover, $E(k)$ is non-negative because of (3). We can obtain a better understanding of turbulence by examining the energy transfer in the wavenumber space.

For inhomogeneous turbulence, the Fourier transform cannot be always used because of complex flow domain and boundaries. Instead of the energy spectrum in the wavenumber space, the second-order structure function $\langle \delta u_i^2(\mathbf{x},\mathbf{r}) \rangle$ [$\delta u_i(\mathbf{x},\mathbf{r}) = u_i(\mathbf{x}+\mathbf{r}) - u_i(\mathbf{x})$] in the physical space can be used to describe the kinetic energy at the length scale of r. The transport equation for the structure function has been examined for several inhomogeneous turbulence (Cimarelli et al., 2013; Cimarelli et al., 2016; Gatti et al., 2020). However, the structure function represents the kinetic energy of eddies with sizes equal to or less than r; it is not the energy density in the scale space. It is more appropriate to introduce the energy density that satisfies (Davidson 2004)

$$K(\mathbf{x}) = \int_0^\infty dr E(\mathbf{x},r) \tag{6}$$

$$E(\mathbf{x},r) \geq 0 \tag{7}$$

where the turbulent energy K at a position is decomposed into the non-negative energy density $E(\mathbf{x},r)$. Using the two-point velocity correlation, the author proposed an expression for the energy density in the scale space (Hamba, 2015; Hamba, 2018). The energy density always satisfies (6), but satisfies (7) only for homogeneous turbulence. It can be negative for inhomogeneous turbulence.

In this work, we improve an expression for the energy density using three filtered velocities (Hamba 2022). The new energy density consists of homogeneous and inhomogeneous parts. The expression can still be negative for inhomogeneous turbulence, but the reason for the negative value can be identified in relation to the turbulence inhomogeneity. We analyze DNS data of turbulent channel flow to examine the homogeneous and inhomogeneous parts of the energy density and investigate the reason for its negative value.

ENERGY DENSITY IN SCALE SPACE

For simplicity, we describe the formulation in the case of one-dimensional filtering. The three-dimensional filtering is described in Hamba (2022). The first filtered velocity is an ordinary one and defined as

$$\overline{u}_i(x,s) = \int_{-\infty}^{\infty} dx' \overline{G}(x-x',s) u_i(x') \tag{8}$$

$$\overline{G}(x-x',s) = \frac{1}{(2\pi s)^{1/2}} \exp\left[-\frac{(x-x')^2}{2s} \right] \tag{9}$$

Here, we adopt a quantity s with a dimension of the square of the length and refer to s as the scale. This filtered velocity represents the velocity with a scale equal to or greater than s.

By differentiating $\overline{u}_i(x,s)$ with respect to s, we can obtain a filtered velocity with a scale equal to s. The second filtered velocity is defined as

$$\hat{u}_i(x,s) \equiv -\frac{\partial}{\partial s} \overline{u}_i(x,s) = \int_{-\infty}^{\infty} dx' \hat{G}(x-x',s) u_i(x') \tag{10}$$

$$\hat{G}(x-x',s) = \frac{1}{(2\pi s)^{1/2}} \left[\frac{1}{2s} - \frac{(x-x')^2}{2s^2} \right] \exp\left[-\frac{(x-x')^2}{2s} \right] \tag{11}$$

The first filtered velocity and the original velocity can be written as

$$\overline{u}_i(x,s) = \int_s^{\infty} ds' \hat{u}_i(x,s'), \quad u_i(x) = \int_0^{\infty} ds \hat{u}_i(x,s) \tag{12}$$

The velocity can be decomposed in terms of $\hat{u}_i(x,s)$ in the scale space. Moreover, the following relationship is obtained.

$$\frac{\partial}{\partial s} \overline{u}(x,s) = \frac{1}{2} \frac{\partial^2}{\partial x^2} \overline{u}_i(x,s), \quad \hat{u}(x,s) = -\frac{1}{2} \frac{\partial^2}{\partial x^2} \overline{u}_i(x,s) \tag{13}$$

By differentiating $\overline{u}_i(x,s)$ with respect to x, we introduce another filtered velocity defined as

$$\tilde{u}_i(x,s) \equiv \frac{\partial}{\partial x} \overline{u}_i(x,s) = \int_{-\infty}^{\infty} dx' \tilde{G}(x-x',s) u_i(x') \tag{14}$$

$$\tilde{G}(x-x',s)) = -\frac{1}{(2\pi s)^{1/2}} \frac{x-x'}{s} \exp\left[-\frac{(x-x')^2}{2s} \right] \tag{15}$$

The third filtered velocity $\tilde{u}_i(x,s)$ is the first derivative of $\overline{u}_i(x,s)$ whereas the second filtered velocity $\hat{u}_i(x,s)$ is the second derivative of $\overline{u}_i(x,s)$.

Using the three filtered velocities, we propose a new expression for the energy density in the scale space. The variance of the first filtered velocity written as

$$\overline{Q}_{ii}(x,s) = \langle \overline{u}_i(x,s) \overline{u}_i(x,s) \rangle \tag{16}$$

represents the kinetic energy of eddies with scales equal to or greater than s. By differentiating $\overline{Q}_{ii}(x,s)$ with respect to s, we can define the energy density $\hat{Q}_{ii}(x,s)/2$, where

$$\hat{Q}_{ii}(x,s) \equiv -\frac{\partial}{\partial s} \overline{Q}_{ii}(x,s) = 2 \langle \hat{u}_i(x,s) \overline{u}_i(x,s) \rangle \tag{17}$$

which satisfies

$$K(x) = \int_0^{\infty} ds \tfrac{1}{2} \hat{Q}(x,s) \tag{18}$$

Using the variance of the third filtered velocity, $\tilde{Q}_{ii}(x,s) = \langle \tilde{u}_i(x,s) \tilde{u}_i(x,s) \rangle$, and the relationship given by (13), we can rewrite the energy density as follows

$$\frac{1}{2} \hat{Q}_{ii}(x,s) = \frac{1}{2} \tilde{Q}_{ii}(x,s) - \frac{1}{4} \frac{\partial^2}{\partial x^2} \overline{Q}_{ii}(x,s) \tag{19}$$

A similar relationship was also used to investigate the stretching of vorticity by the strain rate in Johnson (2020). We call the first and second terms on the right-hand side of (19) the homogeneous and inhomogeneous parts. For homogeneous turbulence, only the homogeneous part remains non-zero; it is clearly non-negative because it is the variance $\tilde{Q}_{ii}(x,s)$. For inhomogeneous turbulence, the energy density can be negative because of the inhomogeneity of the energy $\overline{Q}_{ii}(x,s)$. We can quantitatively examine the deviation from the non-negative part in the case of inhomogeneous turbulence.

ANALYSIS OF CHANNEL FLOW

To investigate the homogeneous and inhomogeneous parts of the energy density, we examine the DNS data of a turbulent channel flow. The size of the computational domain is $L_x \times L_y \times L_z = 2\pi \times 2 \times \pi$, where x, y, and z denote the streamwise, wall-normal, and spanwise directions, respectively. Physical quantities are nondimensionalized by the friction velocity u_τ and channel half width $L_y/2$. The Reynolds number is set to $Re_\tau = 590$.

In this paper, we treat the one-dimensional filtering in the wall-normal direction. The first filtered velocity is written as

$$\overline{u}_i(x,y,z,s) = \int_{-1}^{1} dy' \overline{G}(y,y',s) u_i(x,y',z) \tag{20}$$

The filter function $\overline{G}(y,y',s)$ is basically the same as (9), but it should be modified near the wall. We define $\overline{G}(y,y',s)$ as the solution of the following equation

$$\frac{\partial}{\partial s} \overline{G}(y,y',s) = \frac{1}{2} \frac{\partial^2}{\partial y^2} \overline{G}(y,y',s), \; \overline{G}(y,y',0) = \delta(y-y') \tag{21}$$

with the boundary condition at the wall at $y = \pm 1$. Considering the solenoidal condition for $\overline{u}_i(\mathbf{x},s)$, we adopt the following two sets of boundary conditions:

$$\overline{G} = 0 \text{ for } \overline{u}_x \text{ and } \overline{u}_z, \; \frac{\partial \overline{G}}{\partial y} = 0 \text{ for } \overline{u}_y \tag{22}$$

and

$$\frac{\partial \overline{G}}{\partial y} = 0 \text{ for } \overline{u}_x \text{ and } \overline{u}_z, \; \overline{G} = 0 \text{ for } \overline{u}_y \tag{23}$$

The energy density given by (19) is written as

$$\frac{1}{2} \hat{Q}_{ii}(y,s) = \frac{1}{2} \tilde{Q}_{ii}(y,s) - \frac{1}{4} \frac{\partial^2}{\partial y^2} \overline{Q}_{ii}(y,s) \tag{24}$$

By integrating each term with respect to s, we can obtain an expression for the turbulent energy as

$$K(y) = \int_0^{\infty} ds \frac{1}{2} \tilde{Q}_{ii}(y,s) - \int_0^{\infty} ds \frac{1}{4} \frac{\partial^2}{\partial y^2} \overline{Q}_{ii}(y,s) + \frac{1}{2} \overline{Q}_{ii}(y,\infty) \tag{25}$$

where the right-hand side consists of the homogeneous, inhomogeneous, and residual parts.

First, we plot instantaneous profiles of the filtered velocity to show the effect of the filtering given by (8). Figure 1 shows one-dimensional profiles of the velocity $u_x(x,y,z)$ and the filtered velocity $\overline{u}_x(x,y,z)$ as functions of y at $x = z = 0$ in the case of the second boundary condition for $\overline{G}(y,y',s)$. The scale s is set to 0.0016 for Fig. 1(b) and 0.016 for Fig. 1(c). The scale $s = 0.0016$ corresponds to a filter width $s^{1/2} = 0.04$ normalized by the channel half width. It is clearly seen that the velocity profile become smoother as the scale increases.

Hereafter, we examine profiles of averaged quantities. Figure 2 shows the profiles of the turbulent energy and its three parts given by (25) as functions of y in the case of the first boundary condition for $\overline{G}(y,y',s)$. Except for the near-wall region, the inhomogeneous part is small and the homogeneous part is dominant in Fig. 2(a). However, in Fig. 2(b) where the near-wall region is shown, we can see that the inhomogeneous

part shows a large negative value. The magnitude of both parts is greater than 10 and seems too large compared to the peak value of K $(=4.6)$.

Figure 3 shows the profiles of the turbulent energy and its three parts in the case of the second boundary condition for $\overline{G}(y,y',s)$. The inhomogeneous part shows a negative value near the wall, but its magnitude is much smaller than that in Fig. 2. The turbulent kinetic energy is expressed mainly in terms of its homogeneous part and is slightly modified by its inhomogeneous part near the wall. In this sense, the second set of boundary condition given by (23) is more appropriate. Hereafter, we will show the results given by this boundary condition. The inhomogeneous part involved in (24) is minus the second derivative of the velocity variance. This implies that the negative value of the inhomogeneous part at $y^+<5$ shown in Fig. 3(b) is caused by the concave profile of the turbulent energy near the wall.

Figure 4 shows the contours of the pre-multiplied homogeneous part of the energy density, $s\tilde{Q}_{ii}(y,s)/2$, in the $s-y$ plane. The peak is located at $s=6.5\times10^{-4}$ and $y=-0.94$ ($y^+=35$). The peak location with respect to s increases as y increases. The contour plots are very similar to those of $r_y E(y,r_y)$ given by Hamba (2018). Figure 5 shows the profiles of $s\tilde{Q}_{ii}(y,s)/2$ as functions of s at four y locations. The shift of the peak towards large scales is clearly shown. The value in the case of $y^+=30$ is the largest and this fact corresponds to the peak location of the homogeneous part shown in Fig. 3(b).

Figure 6 shows the profiles of the pre-multiplied energy density and its two parts given by (24) as functions of s at two y locations. In Fig. 6(a) for $y^+=86$, the homogeneous part is positive whereas the inhomogeneous part shows both positive and negative values. Because the inhomogeneous part is not very large, the total value is always positive. In contrast, in Fig. 6(b) for $y^+=2.8$, the inhomogeneous part has a large negative value at $s=10^{-4}$, and the resulting total value also shows a negative value. As discussed before, the large negative value of the inhomogeneous part at $y^+=2.8$ is caused by the concave profile of the turbulent energy near the wall. Therefore, the energy density can be negative in the region very close to the wall because of the inhomogeneous effect.

CONCLUSIONS

A new expression for the energy density in the scale space was proposed using three filtered velocities. The new expression consists of homogeneous and inhomogeneous parts. The homogeneous part is always non-negative whereas the inhomogeneous part is proportional to the second derivative of the velocity variance. DNS data of a turbulent channel flow were used to evaluate the homogeneous and inhomogeneous parts of the energy density and the turbulent energy. It was shown that a concave profile of the filtered-velocity variance at the wall accounts for the negative value of the energy density in the region very close to the wall. In future work, we will examine the energy transfer between different scales using the proposed energy density. It would also be interesting to formulate a statistical theory using filtered velocities to improve the turbulence models.

REFERENCES

Cimarelli, A., De Angelis, E., and Casciola C. M., 2013, "Paths of energy in turbulent channel flows", *J. Fluid Mech.*, Vol. 715, pp. 436-451.

Cimarelli, A., De Angelis, E., Jimenez, J., and Casciola C. M., 2016, "Cascades and wall-normal fluxes in turbulent channel flows", *J. Fluid Mech.*, Vol. 796, pp. 417-436.

Davidson, P. A., 2004, *Turbulence*, Oxford University Press.

Gatti, D., Chiarini, A., Cimarelli, A., and Quadrio M., 2020, "Structure function tensor equations in inhomogeneous turbulence", *J. Fluid Mech.*, Vol. 898, A5 1-33.

Hamba, F., 2015, "Turbulent energy density and its transport equation in scale space", *Phys. Fluids*, Vol. 27, p. 085108.

Hamba, F., 2018, "Turbulent energy density in scale space for inhomogeneous turbulence", *J. Fluid Mech.*, Vol. 842, pp. 532-553.

Hamba, F., 2022, "Scale-space energy density for inhomogeneous turbulence based on filtered velocities", *J. Fluid Mech.*, Vol. 931, A34 1-24.

Johnson, P. L., 2020, "Energy transfer from large to small scales in turbulence by multiscale nonlinear strain and vorticity interactions", *Phys. Rev. Lett.*, Vol. 124, 104501 1-6.

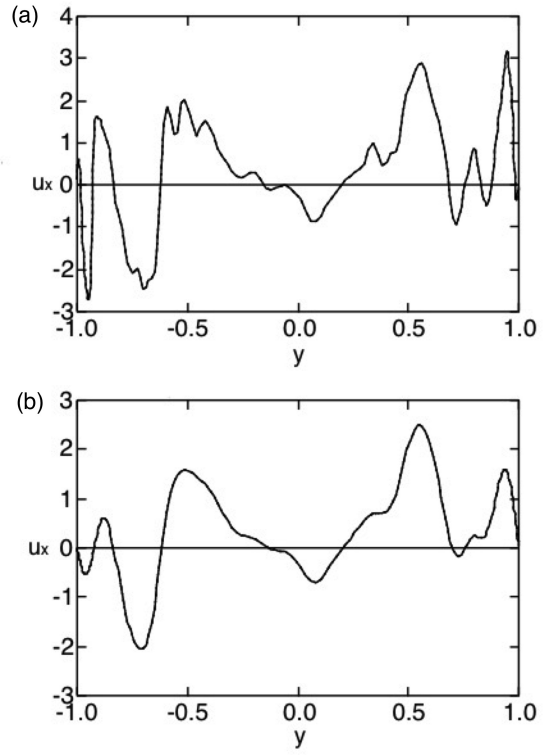

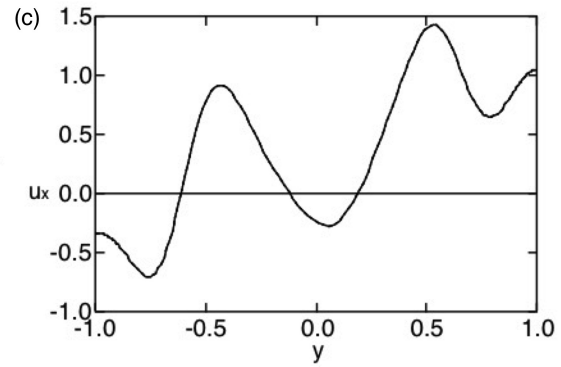

Figure 1. Profiles of velocity $u_x(x,y,z)$ and filtered velocity $\bar{u}_x(x,y,z)$ as a function of y at $x=z=0$ in the case of the second boundary condition for $\bar{G}(y,y',s)$ (a) u_x (b) $\bar{u}_x$ for $s=0.0016$ (c) $\bar{u}_x$ for $s=0.016$

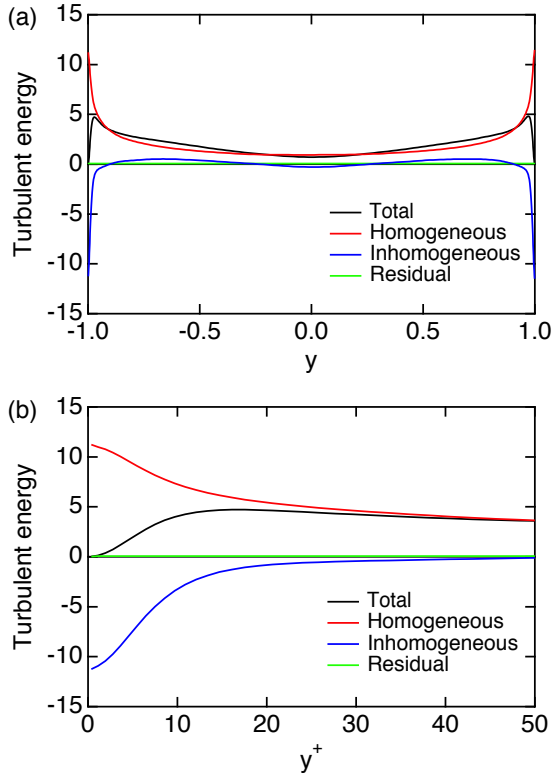

Figure 2. Profiles of turbulent energy K and its three parts given by (25) in the case of the first boundary condition for $\bar{G}(y,y',s)$ (a) $-1\le y\le 1$ (b) $0\le y^+\le 50$

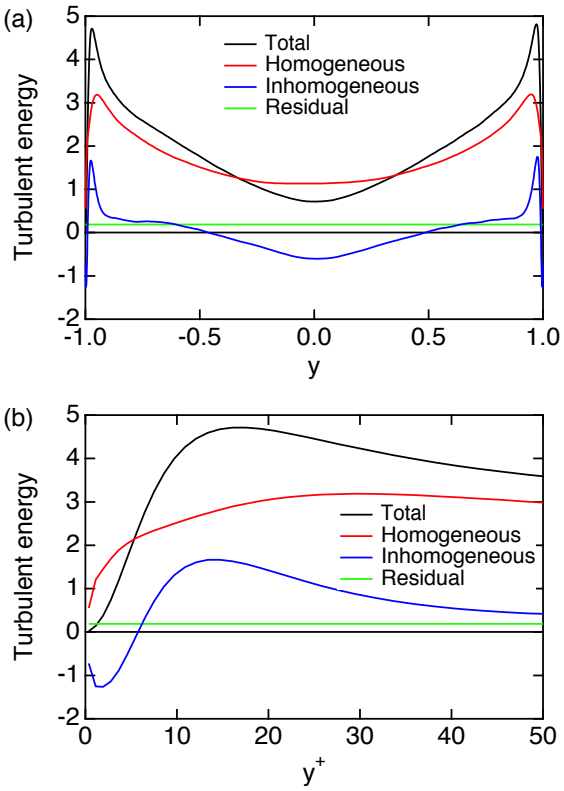

Figure 3. Profiles of turbulent energy K and its three parts given by (25) in the case of the second boundary condition for $\bar{G}(y,y',s)$ (a) $-1\le y\le 1$ (b) $0\le y^+\le 50$.

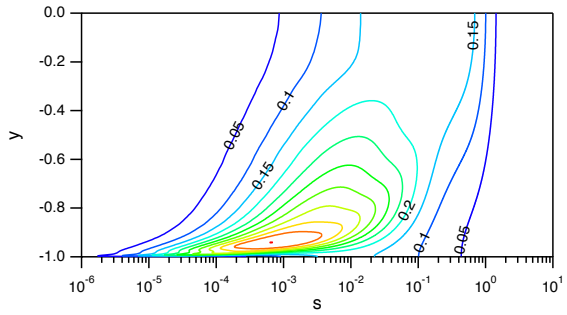

Figure 4. Contour plots of pre-multiplied homogeneous part $s\tilde{Q}_{ii}(y,s)/2$.

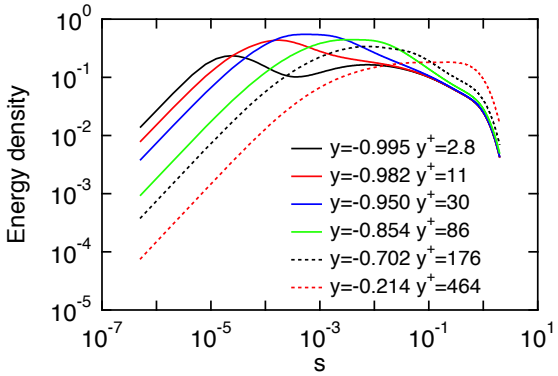

Figure 5. Profiles of pre-multiplied homogeneous part $s\tilde{Q}_{zz}(y,s)/2$ as functions of s.

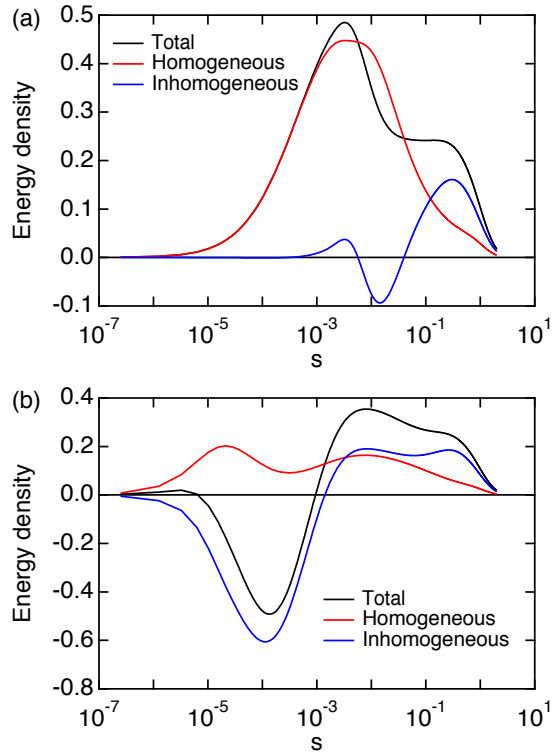

Figure 6. Profiles of pre-multiplied energy density $s\hat{Q}_{ii}(y,s)/2$ and its two parts given by (24) (a) for $y^+ = 86$ and (b) for $y^+ = 2.8$.